



PERGAMON

Available online at [www.sciencedirect.com](http://www.sciencedirect.com)

SCIENCE @ DIRECT®

Solid State Communications 127 (2003) 771–775

solid  
state  
communications

[www.elsevier.com/locate/ssc](http://www.elsevier.com/locate/ssc)

# Optical implementation of entangled multi-spin states in a CdTe quantum well

J.M. Bao<sup>a</sup>, A.V. Bragas<sup>a</sup>, J.K. Furdyna<sup>b</sup>, R. Merlin<sup>a,\*</sup>

<sup>a</sup>FOCUS Center and Department of Physics, The University of Michigan, Ann Arbor, MI 48109-1120, USA

<sup>b</sup>Department of Physics, University of Notre Dame, Notre Dame, IN 46556, USA

Received 25 June 2003; accepted 30 June 2003 by P. Hawrylak

## Abstract

Ultrafast optical pulses and coherent techniques are used to create spin entangled states of non-interacting electrons bound to donors in a CdTe quantum well. Our method, relying on the exchange interaction between optically excited holes and the impurities, can in principle, be applied to entangle a large number of spins. Results are presented for resonant excitation of localized excitons below the gap, and above the gap where the signatures of entanglement are significantly enhanced.

© 2003 Elsevier Ltd. All rights reserved.

PACS: 03.67. – a; 75.50.Pp; 78.67.De; 42.50.Md

Keywords: A. CdTe quantum wells; D. Ultrafast optics; D. Quantum computation; D. Entanglement; D. Spin–flip transitions; E. Raman scattering

## 1. Introduction

The problem of quantum entanglement has attracted much attention since the early days of quantum mechanics. For pure states, entanglement refers to non-factorizable wavefunctions that exhibit non-locality, i.e. correlations that violate Bell's inequalities [1]. Following the proposal by Deutsch for a quantum computer in 1985, the building of a quantum cryptography machine by Bennett et al. in 1989, and the discoveries by Shor in 1994 and by Grover in 1996 of quantum algorithms that outperform those of classical computation, the question of entanglement has now acquired practical significance [1]. Although techniques to entangle two particles and, in particular, two photons [2] have been known for some time, it is only recently that many (up to four)-particle entanglements have been realized [3]. In this work, we propose and demonstrate experimentally a novel method for many-particle entanglement

involving spin states of *non-interacting* paramagnetic impurities in a quantum-well (QW).

## 2. Qubits and entanglement

Our qubits are embodied by Zeeman-split spin states of donor-bound electrons in a Cd<sub>1-x</sub>Mn<sub>x</sub>Te QW [4,5]. The entanglement of Mn<sup>2+</sup>-based qubits is considered elsewhere [5]. Our entanglement procedure draws from an idea put forth by Stühler et al. [6] to explain multiple Mn<sup>2+</sup> spin–flip Raman scattering (RS) in the same system we use to demonstrate the method. The process relies on the exchange interaction between the spin of the impurity electron and excitons that are generated and controlled by optical means. The *N*-electron entangled states relevant to our work are coherent superpositions of the form

$$\psi = \sum_{k=0}^{2S} C_k e^{-ik\Omega_0 t} |S - k\rangle \quad (1)$$

where  $|S - k\rangle$  is the eigenstate of the Zeeman energy operator of eigenvalue  $-g\mu_B B(S - k)$  and  $C_k$  are parameters that can

\* Corresponding author. Tel.: +1-734-763-9759; fax: +1-734-764-5153.

E-mail address: merlin@umich.edu (R. Merlin).

be controlled experimentally. Here  $g$  is the gyromagnetic factor,  $\mathbf{B}$  is the external magnetic field, the direction of which defines the  $x$ -axis, and  $\Omega_0 = g\mu_B B/\hbar$  is the electron spin–flip frequency. The total spin is  $S = N/2$  so that  $\mathbf{S}^2|S - k\rangle = N/2(N/2 + 1)|S - k\rangle$ . Our entanglement procedure is shown schematically in Fig. 1.  $\mathbf{B}_e = \kappa\mathbf{J}$  is an effective magnetic field describing the exchange coupling between the exciton, of energy  $E_e$ , and the impurities,  $\mathbf{J}$  is the spin of the exciton heavy-hole and  $\kappa$  is an exchange constant. The levels involved in Eq. (1) belong to the bottom ladder. In our experiments, the initial non-entangled state is the ground state  $|+S\rangle$  in which the magnetic moments of the electrons are all aligned along  $\mathbf{B}$ . The levels in the upper ladder are eigenstates of  $(\mathbf{B}_e + \mathbf{B})\cdot\mathbf{S}$ , an operator for which the axis of quantization is the  $w$ -axis. Due to a combination of spin–orbit coupling and quantum confinement, the heavy-hole spin and, consequently,  $\mathbf{B}_e$  are parallel to the QW growth axis (the  $z$ -axis) at small external fields [7]. Thus,  $J_z = \pm 3/2$  and, provided  $\mathbf{B}$  is not parallel to the  $z$ -axis, the quantization axes for the bottom and upper states are different and, since the spin is the same, states in different ladders are not orthogonal to each other. It follows that, for an electric-dipole allowed exciton, Raman coherences between arbitrary states in the bottom ladder, say,  $|S - l\rangle$  and  $|S - m\rangle$  can be established by using two laser fields tuned to resonate with  $E_e$  so that their frequency difference is  $|m - l|\Omega_0$ , Fig. 1

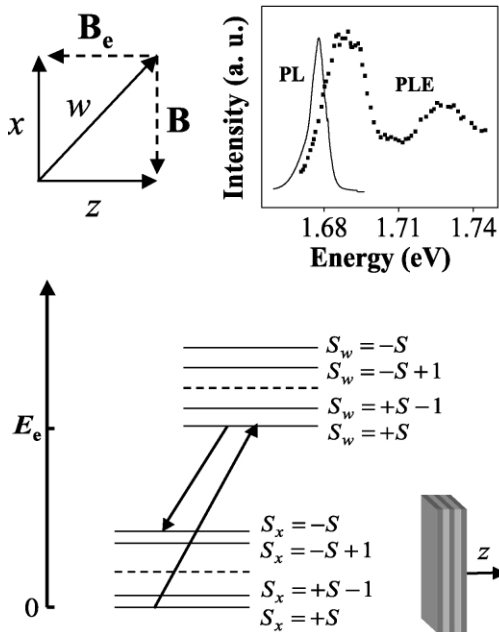


Fig. 1. Generic level structure of a QW system of electrons bound to donors coupled to a localized exciton of energy  $E_e$ . Optical transitions are depicted by arrows.  $\mathbf{B}$  is the external magnetic field and  $\mathbf{B}_e$  is an effective field describing the interaction between the donor electrons and the exciton heavy-hole. The inset shows PL, obtained using the 488 nm line of an Ar-ion laser, and PLE spectra of our sample at  $B = 0$  and  $T = 2$  K.

shows the two transitions leading to the so-called maximally entangled Bell state which is a superposition of the ground  $|+S\rangle$  and the highest excited state  $|-S\rangle$ . We note that a properly tailored optical pulse, involving an infinite set of frequency pairs, can generate a predefined coherent superposition state of the form of Eq. (1) [8]. As it is well known for generic Raman coherences [9], we expect in the limit  $\hbar\Omega_0 \ll E_e$  that the effect of the coherent spin states on the optical properties be that of a modulation involving the harmonics of  $\Omega_0$ . This modulation can be probed in the time domain using standard ultrafast pump-probe methods. We notice that overtones of  $\Omega_0$  should not be observed for non-interacting electrons, and that, because the electron spin is  $s = 1/2$ , the signature for an entanglement of  $N$  electrons is the observation of the  $N$ th harmonic.

### 3. Experiment

Our sample consists of 100 periods of 58-Å-thick  $\text{Cd}_{1-x}\text{Mn}_x\text{Te}$  with 19-Å-thick MnTe barriers grown by molecular-beam-epitaxy on a CdTe substrate along the [001]  $z$ -axis. The manganese concentration is  $x = 0.0039 \pm 0.0004$  [10]. Photoluminescence (PL) and PL-excitation (PLE) spectra are shown in the inset of Fig. 1. The features below  $\sim 1.7$  eV are associated with transitions involving heavy-hole states [5]. The  $\text{Mn}^{2+}$  ions were not intentionally introduced in the wells during growth. Their presence there is due to diffusion from the MnTe-barriers [11]. The sample is nominally undoped. As shown in Fig. 2, however, spin flip RS experiments reveal the presence of a small concentration of donors in the wells [12,13]. Fig. 2 shows Raman data in the Voigt configuration with the laser energy tuned slightly below the PL peak. The fact that the position of the PL is red-shifted (by  $\sim 6$  meV at  $B = 0$ ) with respect to the maximum of the PLE spectrum indicates that the relevant intermediate states of the Raman process are localized

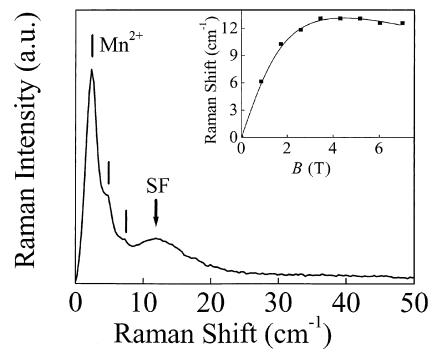


Fig. 2. Resonant Raman spectrum in the Voigt configuration for  $B = 2.6$  T and  $T = 3.5$  K. The laser wavelength is 747 nm. Vertical bars indicate  $\text{Mn}^{2+}$  spin–flip harmonics. The peak labeled SF at  $12 \text{ cm}^{-1}$  is the donor spin–flip. The magnetic field dependence of SF is shown in the inset. The curve is a fit using the Brillouin function.

excitons [5,6]. The narrow peaks below  $\sim 10 \text{ cm}^{-1}$  are due to multiple spin-flips of the  $\text{Mn}^{2+}$  ion ( $s = 5/2$  and  $g \approx 2$ ) while the peak labeled SF is due to the spin-flip of a donor electron. The dependence of the donor spin-flip frequency on the magnetic field is shown in the inset of Fig. 2. The highly non-linear behavior and the saturation at large fields reflect the strong exchange coupling between the donor electrons and the 3d electrons of  $\text{Mn}^{2+}$  which can be described in terms of an effective, enhanced gyromagnetic factor  $g_{\text{EFF}} = g_c - n_0 \alpha \langle S_x \rangle / \mu_B B$  [4]. Here  $g_c \approx -1.64$  is the bare electron  $g$ -factor,  $\langle S_x \rangle = -(5/2)B_{5/2}$  is the average  $\text{Mn}^{2+}$  spin ( $B_{5/2}$  is the Brillouin function) and  $n_0$  is the density of unit cells; for CdTe,  $n_0 \alpha \approx 0.22 \text{ eV}$  [4]. This coupling can be used to determine the  $\text{Mn}^{2+}$ -concentration as well as to distinguish electron spin-flip from other features (note that the  $g$ -factor has approximately the same value for free electrons, electrons bound to donors and electrons in free and bound excitons). Within this context, we observe that, in the Voigt geometry, the shift of the RS feature with magnetic field is exactly a factor of two larger than that of the PL because the Zeeman coupling for the heavy-hole vanishes to lowest order. This does not apply to the Faraday configuration (not shown). In the Faraday geometry, the PL shift is considerably larger reflecting the fact that the exchange interaction between the  $\text{Mn}^{2+}$  spins and the holes is a factor of approximately four larger for electrons [4].

In our time-domain experiments, we used a pump pulse to generate the Raman coherences and a weaker probe pulse to measure the induced change in the reflectivity after a variable time delay [5]. Our mode-locked Ti-sapphire laser (Spectra Physics, Tsunami) provided  $\sim 130 \text{ fs}$  pulses of central energy  $\hbar\omega_C$  in the range 720–840 nm at a repetition rate of 82 MHz. The pump pulse was circularly polarized to excite a single spin component of the heavy hole. The probe pulse was linearly polarized.

Time-domain data for different values of the central energy of the pulses are shown in Fig. 3. The insets show the corresponding Fourier transform spectra, with parameters gained from linear prediction fits [14]. In Fig. 3(a),  $\hbar\omega_C$  is tuned to resonate with the bandgap of the CdTe substrate. The oscillations are due to spin-flip transitions of electrons bound to donors. The frequency of these oscillations depends linearly on the magnetic field with a slope that agrees extremely well with the electron  $g$ -factor in CdTe. As the laser energy approaches the QW gap, at  $\sim 1.68 \text{ eV}$ , the substrate signal gradually decreases while new features due to the QW begin to appear. The results reproduced in Fig. 3(b) correspond to resonant excitation of localized excitons in the QW. The oscillations which persist above  $\sim 15 \text{ ps}$  are associated with the paramagnetic resonance (PR) of the  $\text{Mn}^{2+}$  ions [15]. At short times, the signal is dominated by electron Zeeman quantum beats, i.e. oscillations showing a field- and temperature-behavior consistent with that of spin-flips of electrons. The Fourier spectrum is dominated by the peak labeled SF which is a doublet and appears at the

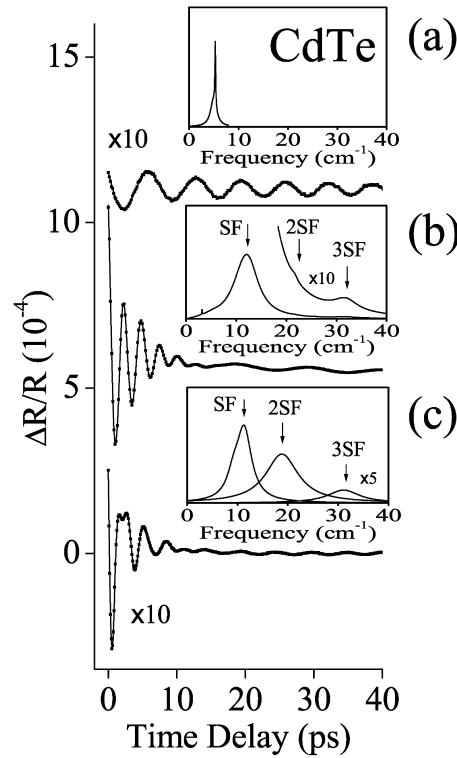


Fig. 3. Differential reflectivity data at (a)  $\hbar\omega_C = 1.60 \text{ eV}$  (below the gap),  $B = 7 \text{ T}$  and  $T = 5 \text{ K}$ . (b)  $\hbar\omega_C = 1.687 \text{ eV}$  (resonance with localized excitons),  $B = 3.4 \text{ T}$  and  $T = 2 \text{ K}$  and (c)  $\hbar\omega_C = 1.71 \text{ eV}$  (above the gap),  $B = 7 \text{ T}$  and  $T = 5 \text{ K}$ . Curves are fits using the linear prediction method [14]. The mode parameters gained from the fits were used to generate the associated Fourier transform spectra depicted in the insets. The main feature in (a) is due to spin-flip of bulk CdTe electrons. In (b), the dominant SF peak is a doublet associated with electron spin-flips [5]. Its lower-frequency component, due to electrons bound to donors, exhibits overtones at twice (2SF) and three times (3SF) the fundamental frequency. The overtones are relatively much stronger in the time-domain data of (c) obtained with excitation above the gap.

same frequency as the homonymous feature in the Raman spectrum of Fig. 2 [5]. The low and high-frequency components of SF are due to the spin-flip of electrons that belong to donors and electrons in the localized excitons, respectively. We note that the SF width is comparable to that of the SF peak in the Raman spectrum (Fig. 2), and that it is considerably larger than that for bulk CdTe spin-flip in Fig. 3(a). The larger spectral width of the QW spin-flip is ascribed to inhomogeneous broadening arising from fluctuations in the manganese concentration [5].

In addition to the single electron spin-flip, and as shown in Fig. 4, the Fourier spectra reveal in a broad range of magnetic fields weaker features, 2SF and 3SF, at nearly twice and three times the frequency of SF. All these modes exhibit a large enhancement when  $\hbar\omega_C$  is tuned to resonate with the localized exciton states [5]. Based on these results,

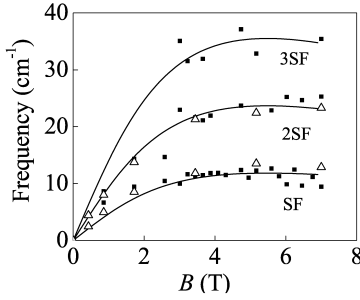


Fig. 4. Magnetic-field dependence of the donor spin-flip harmonics, obtained from time-domain measurements at  $\hbar\omega_c = 1.687$  eV (squares) and  $\hbar\omega_c = 1.71$  eV (triangles). Associated curves are fits using the Brillouin function.

the 2SF and 3SF modes are assigned to multiple spin-flips of donors. As discussed earlier, since the electron spin is  $s = 1/2$  the observation of the SF-overtone indicates the establishment of Raman coherences and, hence, entanglement involving at least three donor impurities [5]. Excitation at energies close to but above the QW gap, leads to an enhancement of the signal of the overtones with respect to the fundamental; see Fig. 3(c). These results clearly indicate that the bound-electron entanglement benefits from the mediation of states in the continuum. However, the process by which the entanglement is attained is not well understood. We note that a mechanism involving the RKKY interaction between localized electrons and delocalized excitons has been previously proposed [16].

Finally, we provide a quantitative estimate of the entanglement for the results in Fig. 3(b) involving resonant excitation of localized excitons. To this end, we neglect absorption and write the effective interaction of light with bound electrons as  $\sum_{S,l} H_S(k, l)$  where

$$H_S(k, l) = E^2(t) \times \left\{ \sum_{\alpha\beta, \eta} e_\alpha e_\beta R_{\alpha\beta}^\eta(k, l) |\eta, S - k\rangle \langle \eta, S - l| + cc \right\} \quad (2)$$

The sum is over *all* sets of  $N(\equiv 2S)$  electrons, each set denoted by  $\eta$ .  $\mathbf{E}$  is the electric field,  $\mathbf{e} = \mathbf{E}/E$  is a unit vector and  $R_{\alpha\beta}^\eta(k, l)$  is the Raman tensor for the corresponding transition of the particular set (this tensor vanishes unless all the impurities in the set interact with a single exciton). Consider a weak impulsive excitation and zero temperature. Then, if  $|+S\rangle$  is the wave function immediately before the pulse strikes (the ground state with all spins aligned along  $\mathbf{B}$ ), integration of Schrödinger equation gives for  $t > 0$  the coherent superposition state

$$\Phi \approx |+S\rangle + iI_0 \sum_{S \geq k > 0, \eta} \Xi_{\eta k} |\eta, S - k\rangle \exp(-ik\Omega_0 t) \quad (3)$$

which is entangled for most values of the integrated intensity of the pump pulse,  $I_0$  [5]. Here,  $\Xi_{\eta k} = (4\pi/n_R c \hbar) \times$

$\sum_{\alpha\beta} e_\alpha e_\beta R_{\alpha\beta}^\eta(k, 0)$  and  $n_R$  is the refractive index. As indicated earlier, a secondary effect of the interaction is that  $\Phi$  leads to time-varying optical constants [9] with concomitant oscillations in the intensity of the reflected probe pulse. Explicitly,

$$\Delta R/R \propto I_0 \sum_{\eta k} |\Xi_{\eta k}|^2 \exp(-ik\Omega_0 t) \quad (4)$$

For a given set of impurities, and to lowest order in  $I_0$ , the only non-zero components of the density matrix operator,  $\hat{\rho}_\eta(k, l) = |\eta, S - k\rangle \langle \eta, S - l|$ , are  $\langle \Phi | \hat{\rho}_\eta(0, 0) | \Phi \rangle \approx 1$  and  $\langle \Phi | \hat{\rho}_\eta(k, 0) | \Phi \rangle = \langle \Phi | \hat{\rho}_\eta(0, k) | \Phi \rangle^* = -iI_0 \Xi_{\eta k} \exp(-ik\Omega_0 t)$ . Let  $N_m$  be the number of sets of  $m$  impurities. Defining the ensemble average  $\rho(m) = \sqrt{\sum_\eta |\langle \Phi | \hat{\rho}_\eta(m, 0) | \Phi \rangle|^2 / N_m}$ , it follows that the amplitude of the  $m$ th-harmonic oscillations gives a direct measure of the entanglement since it is proportional to  $|\rho(m)|^2$ . From the data of Fig. 3(b), we get  $\langle \rho(2) \rangle / \langle \rho(1) \rangle \approx 0.014$  and  $\langle \rho(3) \rangle / \langle \rho(1) \rangle \approx 0.46$ . It is important to realize that the strength of a given harmonic is proportional to the probability of finding the corresponding number of donors in the region where the coupling between the localized exciton and the impurities is significant. Assuming an interaction length of  $\sim 100$  Å (in CdTe, the donor radius is  $\sim 50$  Å), the ratio between the frequency-integrated intensities of the first (SF) and third harmonic (3SF) gives the crude estimate of  $5 \times 10^{16} \text{ cm}^{-3}$  for the density of donors in our sample. Using this density, we obtain  $\langle \rho(1) \rangle / I_0 \approx 30 \text{ m}^2/\text{J}$  which is  $\sim 10^3$ – $10^4$  larger than what a calculation gives for off-resonance excitation.

#### 4. Conclusions

Our results confirm the existence of a system of excitons coupled to paramagnetic impurities in a CdTe QW that is well described by the level structure of Fig. 1. We have shown that such a system can be optically excited to generate multiple spin-flip Raman coherences and that the observation of spin-flip overtones is the signature of a many-impurity entanglement. Experimentally, we used resonant excitation of localized excitons to generate entangled states involving at least three donor impurities. We also showed that the mediation of extended states above the gap facilitates the creation of many-impurity states. In the case of localized excitons, our scheme holds promise for quantum computing applications in that it could be applied to entangle a particular group and, ultimately, a large number of spins by using one exciton at a time to address different sets of impurities.

#### Acknowledgements

Work supported by the NSF under Grants No. PHY 0114336 and No. DMR 0072897, by the AFOSR under

contract F49620-00-1-0328 through the MURI program and by the DARPA-SpinS program. Acknowledgment is made to the donors of The Petroleum Research Fund, administered by the ACS, for partial support of this research. One of us (AVB) acknowledges partial support from CONICET, Argentina.

## References

- [1] See, e.g. M.A. Nielsen, I.L. Chuang, *Quantum Computation and Quantum Information*, Cambridge University Press, Cambridge, 2000.
- [2] P.G. Kwiat, A.J. Berglund, J.B. Altepeter, A.G. White, *Science* 290 (2000) 498.
- [3] C.A. Sackett, D. Kielpinski, B.E. King, et al., *Nature* 404 (2000) 256.
- [4] For a review of diluted magnetic semiconductors, see: J.K. Furdyna, *J. Appl. Phys.* 64 (1988) R29.
- [5] J.M. Bao, A.V. Bragas, J.K. Furdyna, R. Merlin, *Nature Mater.* 2 (2003) 175.
- [6] (a) J. Stühler, G. Schaack, M. Dahl, et al., *Phys. Rev. Lett.* 74 (1995) 2567. (b) J. Stühler, et al., *Phys. Rev. Lett.* 74 (1995) 4966. (c) J. Stühler, et al., *J. Crystal Growth* 159 (1996) 1001.
- [7] R.W. Martin, R.J. Nicholas, G.J. Rees, S.K. Haywood, N.J. Mason, P.J. Walker, *Phys. Rev. B* 42 (1990) 9237–9240.
- [8] (a) W.S. Warren, H. Rabitz, M. Dahleh, *Science* 259 (1993) 1581. (b) I.R. Sola, J. Santamaria, D.J. Tannor, *J. Phys. Chem. A* 102 (1998) 4301.
- [9] R.W. Boyd, *Nonlinear Optics*, Academic Press, San Diego, 1992, pp. 365–397.
- [10] The sample is the same as the one used in Ref. [5] where the value given for the manganese concentration was  $x = 0.003$ . The new, more accurate value was obtained from photoluminescence and Raman scattering measurements using, respectively, the Faraday and Voigt configurations.
- [11] A. Adloff, G. Hendorfer, W. Jantsch, W. Faschinger, *Mater. Sci. Forum* 143–147 (1994) 1409.
- [12] A.K. Ramdas, S. Rodriguez, in: M. Cardona, G. Güntherodt (Eds.), *Light Scattering in Solids VI*, Springer, Berlin, 1991, pp. 137–206.
- [13] R. Meyer, M. Dahl, G. Schaack, A. Waag, *Phys. Rev. B* 55 (1997) 16376.
- [14] (a) H. Barkhuijsen, R. De Beer, W.M.M.J. Bovée, D. van Ormondt, *J. Magn. Reson.* 61 (1985) 465. (b) F.W. Wise, M.J. Rosker, G.L. Millhauser, C.L. Tang, *IEEE J. Quantum Electron.* QE-23 (1987) 1116.
- [15] S.A. Crooker, D.D. Awschalom, J.J. Baumberg, F. Flack, N. Samarth, *Phys. Rev. B* 56 (1997) 7574.
- [16] C. Piermarocchi, P. Chen, L.J. Sham, D.G. Steel, *Phys. Rev. Lett.* 89 (2002) 167402.